

A study of a novel wind turbine concept with power split gearbox

Qian Liu *, Rüdiger Appunn * and Kay Hameyer *

Abstract – This paper focuses on the design and control of a new concept for wind turbines with a planetary gearbox to realize a power split. This concept, where the generated wind power is split into two parts, is to increase the utilization of the wind power and may be particularly suitable for large scale off-shore wind turbines. In order to reduce the cost of the power electronic devices, a synchronous generator, which is driven by the planetary gear, is directly connected to the power grid without electronic converter. A servo drive, which functions as the control actuator, is connected to the power grid by a power electronic converter. With small scale power electronic device, the current harmonics can also be reduced. The speed of the main shaft is controlled to track the optimal tip speed ratio. Meanwhile the speed of the synchronous generator is controlled to stay at the synchronous speed. The minimum rated power of the servo motor and the converter, is studied and discussed in this paper. Different variants of the wind turbine with a planetary gear are also compared. The controller for optimal tip speed ratio and synchronous speed tracking is given.

Keywords: Wind turbine, Power split, Tip-Speed-Ratio, Power split gearbox.

1. Introduction

To improve the utilization of the wind energy, in the last years the size and capacity of a single wind turbine has grown rapidly (5MW to 10MW) for off-shore application. Currently in the wind energy market, the wind turbines with doubly fed induction generator (DFIG) and with direct drive synchronous generator are the most popular small and mid scale wind turbines. However, both of them have technical or economical difficulties for the application on large scale wind turbines. The crucial aspect of the DFIG wind turbines is its small air gap [2]. Meanwhile, the required power level of the power electronic converter for the DFIG wind turbine is about 25% to 30% of the rated power of the wind turbine. On the other hand, the direct drive wind turbines require full scale power electronics, which results in large size, high weight and cost [2].

Besides the machine types, to reduce the cost and the weight of the wind turbine, different gearboxes are studied and implemented. The planetary gearbox is recommended due to its high torque to weight ratio, low backlash, improved efficiency and high resistance to shock [4]. Another advantage of the planetary gearbox is its degree of

freedom between the speed of the sun, ring and carrier compared to the standard gearbox. The power splitting of the planetary gearbox and its freedom of speed have been widely used in vehicles and robotics [5-7]. It is possible that one of the terminals of the planetary gearbox can rotate with a constant speed while the other two are speed controlled.

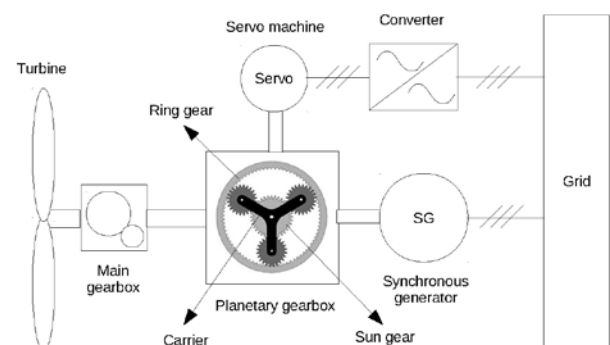


Fig. 1. : Example structure of a wind turbine with planetary gearbox.

With this idea, a new concept of the wind turbine with a planetary gearbox is proposed in [1] [3]. Fig.1 shows the structure of the wind turbine. The turbine is connected to a main gearbox. A synchronous generator is connected to the planetary gear box and directly to the power grid without any power electronic devices; a servo machine is working as the control actuator of the planetary gearbox, which is connected to the power grid with a converter. The main

* Institute of Electrical Machines (IEM), RWTH Aachen University, Germany. (qian.liu@iem.rwth-aachen.de)

benefit of this structure is the requirement of a small scale converter for the servo machine to reduce the cost of the wind turbine and improve the quality of the current. Another aspect is that the avoidance of the slip-ring reduces the failure rates of the wind turbine when compared to DFIG wind turbines. The optimal tip speed ratio of the turbine and the synchronous speed of the synchronous generator can be achieved by the control of the servo machine. In [1], the general operation of the wind turbine with power split device and the model of the planetary gear box are shown. In [3] some analysis of the power split and the choice of the servo machine are discussed. Besides, an example controller is also described to achieve the functionality of the wind turbine. Based on the literature mentioned above, the configuration of the wind turbine with power split devices is considered in our study for a minimum power split of the servo machine.

In this paper, section 2 presents the aerodynamics and the power curve of a wind turbine. The minimum rated power of the servo machine and the configuration of the gearboxes to achieve the functionality of the optimal tip speed ratio and the synchronous speed tracking are discussed in section 3. Due to the producibility limitation of the gear ratio of the gearboxes, three parameters are considered for the variation of the wind turbine: the gear ratio of the main and planetary gearboxes and the speed range of the main shaft. In section 4, different variants of the wind turbine with a planetary gear are discussed and compared. In section 5, a simple control strategy is given to improve the performance of the wind turbine. The simulation structure and the controller of the servo machine are also presented in section 6 to verify the optimal wind power extraction and the frequency variation of the synchronous generator.

2. Wind energy and power curve of a wind turbine

One of the key points of the wind turbines is to obtain more kinetic energy from the wind. The extracted wind power can be presented by the following equation [8]:

$$P_{mech} = \frac{\rho}{2} C_p(\lambda, \beta) A_t V_w^3 \quad (1)$$

where ρ is the air density; A_t is the area covered by the turbine rotor; V_w is the wind speed; C_p is the power coefficient which is a function of the tip speed ratio λ and the pitch angle β . The description of the power coefficient is discussed in literature [8] [10]. The optimal value of the power coefficient is reached when the tip speed ratio is constant. In order to generate the maximum energy from the wind, the turbine speed has to be controlled to keep the tip speed ratio constant (optimum value).

To extract more power out of the wind, it is preferred, that the wind turbine stays at the optimal tip speed ratio in a wide speed range. The mechanical power curve of a wind turbine is shown in [9] [10]. An example power curve of a

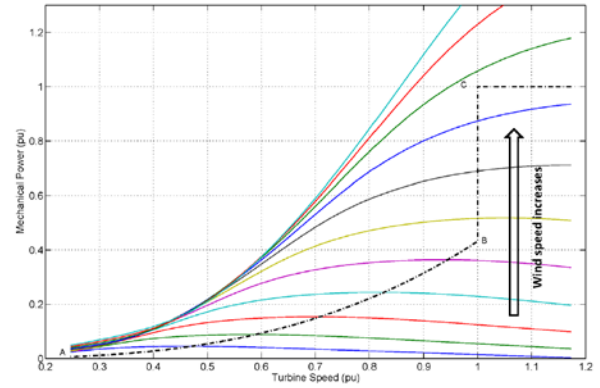


Fig. 2. : Typical power curve of a variable speed wind turbine.

variable speed wind turbine with rated power 850kW and rated wind speed 16m/s is shown in fig.2. The curves with wind speed 4m/s to 14m/s show the power which can be obtained from the wind at different wind speed and turbine speed. The slashed curve shows the actual wind power delivered to the wind turbine. Three operating points are important for the wind turbine: A presents the cut-in operation; B is the operating point where the rated speed of the turbine is reached and the pitch control starts to be activated; C is the operating point that both rated speed and rated power of the turbine are reached. When the turbine speed is below its maximum speed (curve A to B in fig.2), the wind turbine is operating in the optimal power region where the tip speed ratio is controlled to its optimum value. When the turbine speed reaches its maximum value and the wind speed still increases, the turbine speed is controlled to stay at its rated value and the extracted wind power increases until the rated power is reached (curve B to C in fig.2). When the operating point C is reached and the wind speed still increases, the wind turbine is mainly controlled by the pitch controller to keep the turbine at its rated power and rated speed.

Table 1. Variants of the wind turbine with planetary gear.

Variants	Main shaft	Syn. Generator	Servo Machine
A	Carrier	Sun	Ring
B	Carrier	Ring	Sun
C	Sun	Carrier	Ring
D	Sun	Ring	Carrier
E	Ring	Carrier	Sun
F	Ring	Sun	Carrier

3. Power splitting of the wind turbine

The power splitting of the wind turbine is achieved by a

planetary gearbox, which has three terminals: sun, ring and carrier wheel. For the novel concept of power split wind turbine, the turbine, synchronous generator and servo machine can be connected to each of these three terminals respectively. Therefore, there are 6 different variants as shown in Table 1. Since the analysis for these 6 variants are almost the same, without loss of generality. In this section we take the variant B as an example: the main shaft is connected to the carrier; the synchronous generator is connected to the ring gear and the servo machine is connected to the sun gear.

3.1 Model of the planetary gear

To analyze the delivered mechanical power to the servo machine, the stationary model is chosen in this section, which can be found in literature [1] [3]. The constraints of the speed and torque for a planetary gearbox are shown by the following equations:

$$(1-i_0)\omega_c = \omega_s - i_0\omega_r \quad (2)$$

$$T_s = -\frac{1}{1-i_0}T_c \quad (3)$$

$$T_r = \frac{i_0}{1-i_0}T_c \quad (4)$$

where ω and T are the rotational speed and torque and the subscript s, r and c present the sun, ring and carrier respectively. i_0 is the gear ratio between the ring gear and sun gear, which is defined as:

$$i_0 = -\frac{Z_r}{Z_s} \quad (5)$$

where Z_r and Z_s are the radius of the ring and sun gear respectively. Therefore, the gear ratio $i_0 < -1$. In the industry, the gear ratio of a producible planetary gear is limited to $-9 < i_0 < -2$. The rated torque of a planetary gear is also influenced by the gear ratio. The highest rating of a planetary gear can be achieved at a balanced torque distribution with $i_0 = -4$.

3.2 Optimal power splitting for the servo machine

To reduce the rating of the servo machine and the corresponding converter, the peak power delivered to the servo machine (both in motor and generator mode) is expected as small as possible when the rated torque of the wind turbine is fixed. In order to study the minimum rated power of the servo machine, in this paper the losses of the gearboxes are neglected and the steady state characteristics are considered. Before the analysis, some parameters are defined in the following:

- Synchronous speed ω_1 , which is the synchronous

speed of the synchronous generator.

- The gear ratio of the main gearbox xG_0 . Here G_0 is a constant so that the rated speed of the turbine can be transformed to the synchronous speed ω_1 at the main shaft. x is a variable scale to be determined.
- $\Delta\omega$ is the normalized speed variation of the main shaft, where the base value is the synchronous speed.

To minimize the power splitting of the servo machine, the parameters of the wind turbine, which considered as variables are x , i_0 and $\Delta\omega$. With the defined parameters, the main shaft speed, which is also the carrier speed, can be rewritten as:

$$\omega_c = x\omega_1(1 + \Delta\omega) \quad (6)$$

with $\Delta\omega \in (-1,0]$. Therefore, the extracted wind power from equation (1) can be rewritten as:

$$P_c = K(\lambda, C_p)\left(\frac{\omega_c}{x}\right)^3 = K(\lambda, C_p)[\omega_1(1 + \Delta\omega)]^3 \quad (7)$$

here $K(\lambda, C_p)$ is a function of the tip speed ratio λ and power coefficient C_p . As shown in the previous section, due to the operated power curve of the wind turbine, the optimal power coefficient and tip speed ratio can be realized when the turbine speed is less than its maximum value (curve A to B in fig.2). Therefore, the coefficient $K(\lambda, C_p)$ is a constant K_0 in this situation. Using (7), the mechanical power delivered to carrier is:

$$P_c = K_0[\omega_1(1 + \Delta\omega)]^3 \quad (8)$$

The ring gear is always controlled to rotate at synchronous speed due to the synchronous generator. Since the transient dynamics are not considered in this analysis, it is assumed that the ring gear has a constant angular speed ω_r . Using (2) (3) and (8), the mechanical power delivered to the sun gear can be calculated:

$$P_s = -K_0\omega_1^3(1 + \Delta\omega)^2 \left[(1 + \Delta\omega) + \frac{i_0}{x(1 - i_0)} \right] \quad (9)$$

After the turbine speed reaches its maximum value and if the wind speed still increases, the speed of the wind turbine is kept at its rated speed, which is a known constant (on the power curve B to C in fig.2). Therefore, the mechanical power delivered to the carrier is expressed as:

$$P_c = K(\omega_1, \lambda, C_p)\omega_1^3 \quad (10)$$

where $K(\omega_1, \lambda, C_p)$ is larger than K_0 and is strictly increasing when the wind speed increases. Denote K_{max} as the maximum value of $K(\omega_1, \lambda, C_p)$, which results in the rated power of the wind turbine. Using (2) (3) and (10) the mechanical power delivered to the sun gear is:

$$P_s = -K(\omega_1, \lambda, C_p) \omega_1^3 \left(1 + \frac{i_0}{x(1-i_0)}\right) \quad (11)$$

The servo drive can be operated in motor and generator modes. From (9) and (11), it can be noticed that the peak value of the mechanical power to the sun gear depends on the gear ratios of the gearboxes (negative power means generator mode and positive power means motor mode). The optimal mechanical power delivered to the servo machine is expressed as $P_{opt} = \min\{\max\{|P_s|\}\}$.

To find the minimum mechanical power of the servo machine, we only have to consider the peak power in both motor and generator modes (equation (9) and (11) respectively). The extreme value of equation (11) is:

$$P_{s1}^{ext} = -K_{max} \omega_1^3 \left(1 + \frac{i_0}{x(1-i_0)}\right) = -\left(1 + \frac{i_0}{x(1-i_0)}\right) P_{rated} \quad (12)$$

where P_{rated} is the rated power of the turbine. The extreme value of equation (9) is:

$$P_{s2}^{ext} = \frac{4}{27} K_0 \omega_1^3 \left(\frac{-i_0}{x(1-i_0)}\right)^3 = \frac{4}{27} \frac{K_0}{K_{max}} \left(\frac{-i_0}{x(1-i_0)}\right)^3 P_{rated} \quad (13)$$

when the following relationship holds:

$$a = \frac{-i_0}{x(1-i_0)} < 1.5 \quad (14)$$

Considering the minimum value P_{opt} with different configurations in (9) to (14): $0 < a < 1$, $1 \leq a \leq 1.5$ and $a > 1.5$. P_{opt} can be reached in the region $0 < a < 1$ with $P_{opt} = |P_{s1}^{ext}| = |P_{s2}^{ext}|$. Therefore, the optimum configuration also depends on the power characteristic of the turbine, which in details is depending on $b = K_0 / K_{max}$. Finally we have $P_{opt} = (1-a)P_{rated}$ and a is the solution of the equation $4by^3 = 27(1-y)$ within the region $0 < y < 1$.

The parameter b determines the region of the partial load with optimal tip speed ratio. The larger b is, the region of the partial load with optimal tip speed ratio is also larger. However, the minimum mechanical power delivered to the servo drive is also larger. For example, when the optimal tip speed region extends from cut-in to rated operating point $b = 1$ holds, the minimum power of the servo machine $P_{opt} = 0.106P_{rated}$ with $a = 0.894$. In another case, when $b = 0.432$ (the power curve in fig.2), $P_{opt} = 0.054P_{rated}$ with $a = 0.946$.

Therefore, a compromise has to be made between the optimal tip speed ratio region and the power level of the servo machine. Since there is still one degree of freedom in the gear ratios of the main and planetary gears to meet the optimum configuration, it is possible to choose the gear ratio within the producible region that $-9 < i_0 < -2$. With

the minimum power delivered to the servo machine, the power rating of the converter can be minimized, which results in small size and low cost.

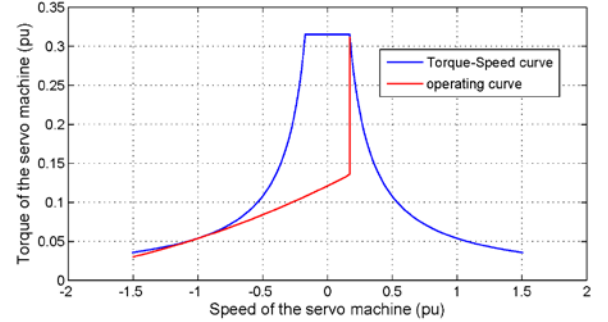


Fig. 3: Operating and torque-speed characteristic of the servo machine.

After the parameter a of the gearboxes are determined, from (2) to (6), the speed and torque range of the servo machine can be expressed by the following equations:

$$\omega_s = -i_0 \omega_1 \left(\frac{1-a}{a} + \frac{1}{a} \Delta\omega\right) \quad (15)$$

$$T_s = -\frac{a}{i_0} T_c^* \quad (16)$$

where T_c^* is the torque when the variable $x = 1$, which is strictly increasing along the power curve. With equations (15), (16) and the power characteristic of the turbine, the operating curve of the servo machine can be fixed. In fig. 3 the red line shows an example operating characteristic of the servo machine for variant B with power characteristic in fig. 2. The gear ratio of the wind turbine i_0 is chosen to -3. From (15), (16) and fig. 3, it can be noticed that the rated operating point with minimum rated power of the servo machine is reached at $\Delta\omega=0$, where the corresponding torque-speed characteristic of the servo machine is shown by the blue characteristic in fig. 3. The maximum permissible speed of the servo machine is determined by the $\Delta\omega$, which is determined by the cut-in wind speed and the wind speed when the rated speed of the turbine is arrived (at point B in fig. 2). The ratio between the maximum permissible speed and the rated speed of the servo machine is invariant with the gear ratio and is relatively large. Therefore, for minimum power split, a good field weakening capability of the servo machine is required. To loose the difficulty of field weakening for the machine design, the rated speed of the servo machine can be increased while the rated torque remains unchanged.

4. Variants of the wind turbine with power split

As mentioned in the last section (in table 1), due to the different connection of the planetary gear, there are 6 variants for the wind turbine with power split. Using the

same analysis method in section 3, we can find out that if the power ratio b in the power characteristic of the wind turbine is fixed, the minimum peak mechanical power delivered to the servo machine is the same for all variants mentioned in table 1. However, different conditions of the gear ratios of the main and planetary gear boxes have to be fulfilled to reach the minimum power split.

Table 2. Minimum power split for all variants.

Variants	Minimum power split	Condition
A	$P_{servo} = (1 - a)P_{rated}$	$\frac{1}{(1 - i_0)x} = a$
B	$P_{servo} = (1 - a)P_{rated}$	$-\frac{i_0}{(1 - i_0)x} = a$
C	$P_{servo} = (1 - a)P_{rated}$	$\frac{1 - i_0}{i_0x} = a$
D	$P_{servo} = (1 - a)P_{rated}$	$-\frac{i_0}{i_0x} = a$
E	$P_{servo} = (1 - a)P_{rated}$	$-\frac{1 - i_0}{i_0x} = a$
F	$P_{servo} = (1 - a)P_{rated}$	$-\frac{1}{i_0x} = a$

Table 3. Torque and speed of the servo machine with minimum power split.

Variants	Speed of the servo machine	Torque of the servo machine
A	$\omega = -\frac{\omega_1(1 - a + \Delta\omega)}{i_0a}$	$T = -ai_0T_c^*$
B	$\omega = -\frac{i_0\omega_1(1 - a + \Delta\omega)}{a}$	$T = -\frac{a}{i_0}T_c^*$
C	$\omega = -\frac{(1 - i_0)\omega_1(1 - a + \Delta\omega)}{i_0a}$	$T = -\frac{ai_0}{1 - i_0}T_c^*$
D	$\omega = -\frac{i_0\omega_1(1 - a + \Delta\omega)}{(1 - i_0)a}$	$T = -\frac{a(1 - i_0)}{i_0}T_c^*$
E	$\omega = \frac{(1 - i_0)\omega_1(1 - a + \Delta\omega)}{a}$	$T = \frac{a}{1 - i_0}T_c^*$
F	$\omega = \frac{\omega_1(1 - a + \Delta\omega)}{(1 - i_0)a}$	$T = a(1 - i_0)T_c^*$

Table 2 shows the formulas of the minimum power split of the servo machine and the corresponding configuration. Here, the value of a is the solution of the equation $4by^3 = 27(1 - y)$ within the region $0 < y < 1$.

Since the gear ratios of the main and planetary gear boxes are different for all the variants to reach the minimum power split, the torque and speed ranges of all variants are different. Table 3 shows formulas for the torque and speed of the servo machine for all variants. All the parameters are

defined the same as in section 3. As mentioned in the previous sections, a is usually larger than 0.9 and $-9 < i_0 < -2$, the comparison between the torque of the servo machine for all variants is: $F > A > D > C > B > E$. Considering the volume and cost of the servo machine, only variant B and E suit for the implementation in the reality. The comparison between the maximum speed of the servo machine is inverted: $E > B > C > D > A > F$. With the same reason for variant B, a good field weakening capability of the servo machine for all other variants is also required.

5. Control of the servo machine

In the new wind turbine concept, the functionalities of the optimum tip speed ratio tracking and the synchronization of the synchronous generator are realized by the servo machine. A control structure of the servo machine is shown in [3], which is a speed controller of the servo drive. In this paper, the controller of the servo machine consists of a parallel structure of two PI controllers, which can have different gains. One PI controller controls the speed of the main shaft to track the power curve of the turbine. Meanwhile the other controls the speed of the synchronous generator to be synchronous speed. Here, we take variant B as the example.

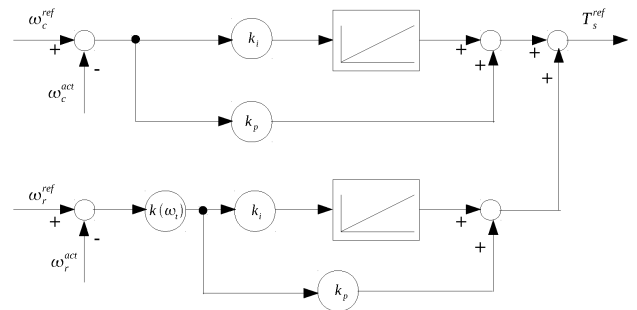


Fig. 4: Time variant parallel controller of the servo machine.

Fig.4 shows the parallel structure of the controller of the servo machine. The parameters of the power characteristic controller (PI controller on the lower side) and the synchronous speed controller (PI controller on the upper side) have different gain $k(\omega_s)$, which depends on the turbine speed. At low wind speed, the synchronization of the synchronous generator is more critical than the optimal tip speed ratio tracking, the weighting of the synchronization controller should be larger than the other. The parameters of the controller can also be a variable of the turbine speed. When the turbine speed reaches its maximum value, the gain of the power curve controller can be enlarged to prevent the turbine from accelerating when a wind gust arrives. The performance of the parallel controller is shown in the next section.

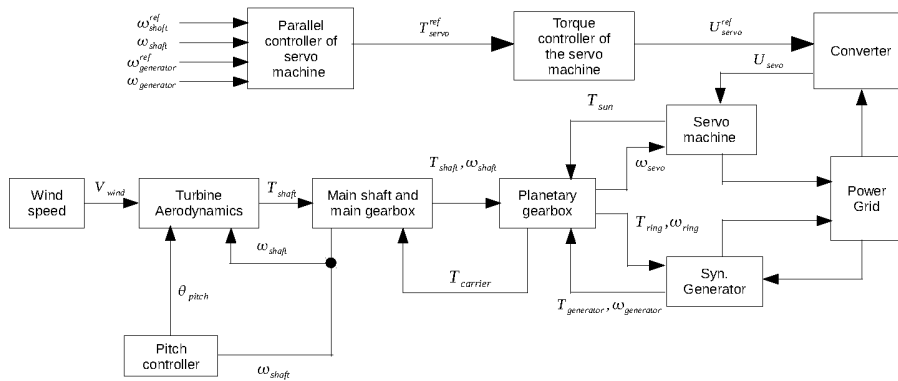


Fig. 5: Simulation structure of the wind turbine with planetary gearbox.

6. Simulation results

The simulation of the power split wind turbine with the proposed configuration and control strategy is implemented in Matlab/Simulink. The simulation is made with variant B, whose simulation structure is shown in Fig.5. The wind turbine is modeled with rated power 855 kW and rated wind speed 16 m/s. The power curve of the turbine is implemented with the curve shown in fig.2. The models of the planetary gearbox and the synchronous generator with 2 pole pairs are utilized from the SimDrive and SimPower Toolboxes (Matlab Toolbox) respectively. According to the optimization of the wind turbine in the previous section ($a = 0.946$), the configurations of the turbine and rated values of the servo machine are designed for minimum power split and collected in table 4 (with base speed 1500 rpm and base power 855 kW).

Table 4. Specifications of the wind turbine.

Specification	Value
Ratio of the planetary gearbox i_0	-3
Max. speed of the main shaft	0.793 pu
Synchronous speed	1 pu
Max. power of the sun gear	0.054 pu
Rated speed of the servo machine	0.171 pu
Rated Torque of the servo machine	0.315 pu

In the simulation, the servo machine is chosen as an induction machine whose torque is limited by the given rated torque in table 4 and the field weakening is implemented. The steady state behavior of the wind turbine is first simulated with constant wind speed from 4 m/s to 18 m/s. The speed and power of the sun gear, ring gear and the carrier are shown in fig. 6. It is shown that the speed variation of the sun gear is almost proportional to the speed variation of the carrier with factor i_0 . When the wind speed is small, the servo machine is working in motor mode. When the wind speed increases, the servo machine is switched to the generator mode. From the power curves in fig. 6, it is shown that the peak power delivered to the sun gear is 0.054 pu in both motor and generator modes, which

proves the analysis in the previous sections. It can also be mentioned, with such configurations of the wind turbine, the servo machine has small rated speed but large speed variation range. So the induction machine is more suitable than the synchronous machine due to its excellent field weakening characteristics.

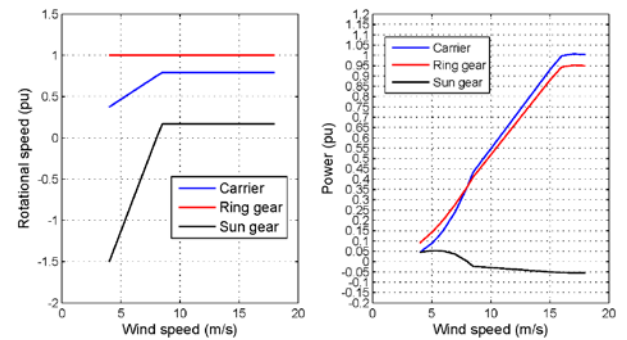


Fig. 6: Simulation results with different wind speed in steady state.

Fig. 7 shows the power characteristics of the wind turbine depending on the turbine speed. The power curve of the carrier fits the power curve of the turbine shown in fig. 2 yet the maximum power of the sun gear is limited to the optimum value 0.054 pu.

The transient behavior of the mentioned wind turbine with optimal power splitting is investigated by the simulation with time variant wind speed. The wind speed is shown in fig. 8, which is almost from 4 m/s to 18 m/s. The study of the optimal tip speed ratio and the synchronous speed tracking are collected in fig. 9. The reference speed of the main shaft according to the power curve in fig. 2 is shown by the red line in fig. 9 on the upper side. The dark and light blue curves show the speed of the main shaft with the constant controller shown in [3] and with the time varying parallel controller described in this paper. It can be noticed that both controllers can track the reference value. At the high wind speed range, the speed of the main shaft has fewer oscillations when controlled by the time varying parallel controller, which is a benefit for the mechanical system. The dashed and dot-dashed curves in the figure on

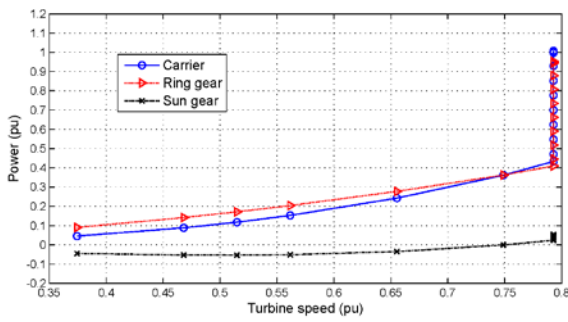


Fig. 7: Simulation results of the power curve.

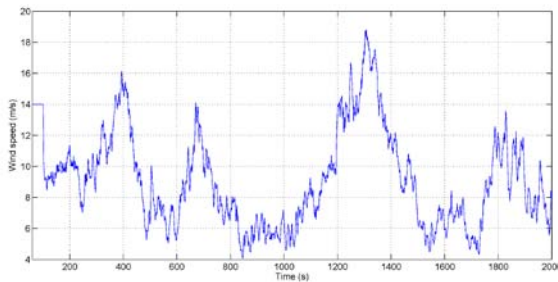


Fig. 8: Wind speed for the simulation.

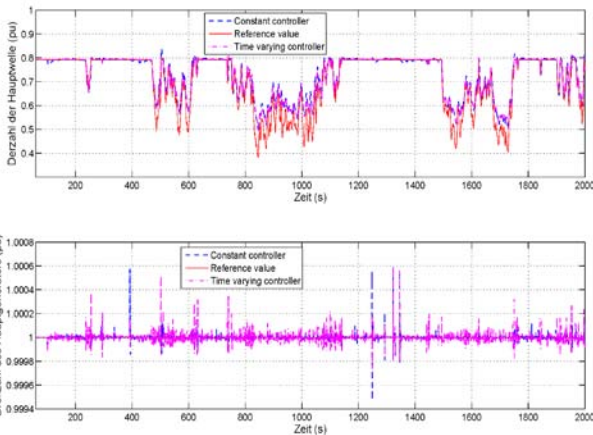


Fig. 9: Speed of the main shaft and the synchronous generator.

the lower side in fig. 9 show the speed of the synchronous generator. It is shown that the speed of the synchronous generator has quite small oscillation for both controllers under strong wind variation. It can be concluded that the wind turbine with optimum power split can track the power characteristic and the synchronous generator can be directly connected to the power grid.

Fig. 10 shows the simulation results of the power and torque of the main shaft, synchronous generator and the servo machine. The power and torque of the servo machine are limited to the designed rated values. However, the functionality of the wind turbine can still be achieved even when a wind gust appears. Fig. 11 shows the speed variation of the servo machine when the wind changes from 4 m/s to 18 m/s in less than 300 seconds. The speed of the servo machine almost stays at its rated speed when the maximum speed of the main shaft is reached. On the other

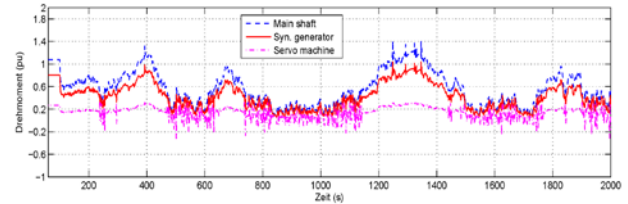
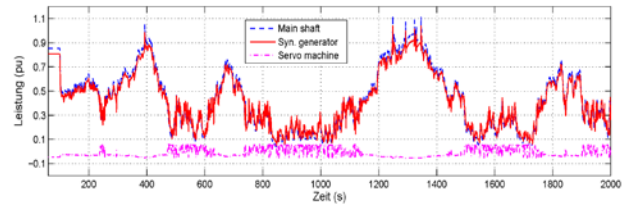


Fig. 10: Power and torque of the wind turbine.

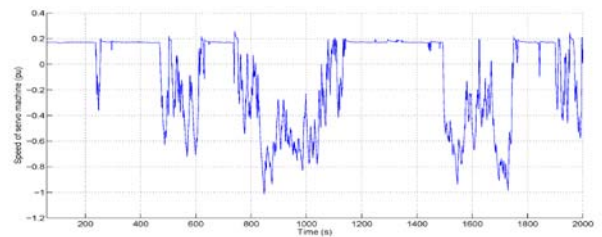


Fig. 11: Speed of the servo machine.

hand, the speed variation with time variance wind is smaller than it in steady state (in fig. 6) due to the damping of the mechanical inertia. However, the speed variation of the servo machine is very large compared to its rated speed. So the induction machine fits the servo machine better when compared to the PMSM.

7. Conclusion

This paper presents the structure of a novel concept wind turbine with a planetary gearbox for a power split operation. The best configuration of the wind turbine is studied for the optimum power split, which is also the minimum power rating of the converter required by the servo machine. The torque and speed ranges of the servo machine corresponding to the best configuration are given for the design of the servo machine. The minimum power split for different wind turbine variants of the wind turbine is discussed and compared. The torque level and speed range of the servo machine for different wind turbine variants are shown to choose a suitable structure for buildup. A time variant parallel controller is discussed in this paper to track the optimum speed ratio and the synchronous speed. The validation of the optimum power split and the speed tracking is demonstrated by the simulation, where the optimum configuration can achieve the mentioned functionality and the time varying parallel controller shows better performances at high wind speed. The speed range of the servo machine is shown, which indicates that, the induction machine has advantages for the servo machine compared to the PMSM. The next step of the study is to

build up a test bench for the measurement of the mentioned wind turbine with power split.

Acknowledgements

This work is supported by the Ziel-2-Programm NRW 2007-2013 "Regionale Wettbewerbsfähigkeit und Beschäftigung" (EFRE).

References

- [1] Xiaoming Rui; Lin Li; Ximei Li, "Fundamentals of a power splitting driving chain for large wind turbines," *Intelligent Control and Automation, 2008. WCICA 2008. 7th World Congress on*, vol., no., pp.9347,9350, 25-27 June 2008.
- [2] Delli Colli, V.; Marignetti, F.; Attaianese, C., "Analytical and Multiphysics Approach to the Optimal Design of a 10-MW DFIG for Direct-Drive Wind Turbines," *Industrial Electronics, IEEE Transactions on*, vol.59, no.7, pp.2791,2799, July 2012.
- [3] Caselitz, p., Grebe, R., Krueger, T., Pischel, K., Schoo, A., "Drehzahlvariable Windkraftanlagen mit elektrischer geregelter Ueberlagerungsgetriebe", *Deutsche Windenergie-Konferenz (DEWEK)*, pp.171-175, 1992.
- [4] Daneshi-Far, Z.; Henao, H.; Capolino, G.-A., "Planetary gearbox effects on induction machine in wind turbine: Modeling and analysis," *Electrical Machines (ICEM), 2012 XXth International Conference on*, vol., no., pp.1790,1796, 2-5 Sept. 2012.
- [5] Szumanowski, A.; Yuhua, C.; Piorkowski, P., "Analysis of different control strategies and operating modes of compact high planetary transmission drive," *Vehicle Power and Propulsion, 2005 IEEE Conference*, vol., no., pp.7 pp., 7-9 Sept. 2005.
- [6] Xiaowu Zhang; Chiao-Ting Li; Dongsuk Kum; Huei Peng, "Prius+ and Volt-: Configuration Analysis of Power-Split Hybrid Vehicles With a Single Planetary Gear," *Vehicular Technology, IEEE Transactions on*, vol.61, no.8, pp.3544-3552, Oct. 2012.
- [7] Hoyul Lee; Youngjin Choi, "A New Actuator System Using Dual-Motors and a Planetary Gear," *Mechatronics, IEEE/ASME Transactions on*, vol.17, no.1, pp.192-197, Feb. 2012.
- [8] Slootweg, J.G.; Polinder, H.; Kling, W.L., "Dynamic modelling of a wind turbine with doubly fed induction generator," *Power Engineering Society Summer Meeting, 2001*, vol.1, no., pp.644-649 vol.1, 2001.
- [9] Papathanassiou, S.A.; Papadopoulos, M.P., "Dynamic behavior of variable speed wind turbines under stochastic wind," *Energy Conversion, IEEE Transactions on*, vol.14, no.4, pp.1617-1623, Dec 1999.
- [10] Ackermann, Thomas, "*Wind Power in Power Systems*", John Wiley and Sons, 2005, pp.526-531.



Qian Liu finished his Bachelor in Electrical Engineering in 2008 at Shanghai Jiao Tong University, China. In 2011 he received his Master degree in Control Engineering from Technical University of Kaiserslautern, Germany. Currently he is a research associate in the Institute of Electrical Machines at RWTH Aachen University, Germany. His research focuses on wind turbines, motor drive system and power electronics.



Rüdiger Appunn received the diploma in electrical engineering from the Faculty of Electrical Engineering and Information Technology, RWTH Aachen University, Aachen, Germany, in 2008. Since 2008, he has been a researcher with the Institute of Electrical Machines, RWTH Aachen University. His research fields include magnetic levitation, mechatronics and inductive power transmission.



Dr. Kay Hameyer (FIET, SMIEEE) received his M.Sc. degree in electrical engineering from the University of Hannover and his Ph.D. degree from the Berlin University of Technology, Germany. After his university studies he worked with the Robert Bosch GmbH in Stuttgart, Germany as a Design Engineer for permanent magnet servo motors and vehicle board net components. Until 2004 Dr. Hameyer was a full Professor for Numerical Field Computations and Electrical Machines with the KU Leuven in Belgium. Since 2004, he is full professor and the director of the Institute of Electrical Machines (IEM) at RWTH Aachen University in Germany. 2006 he was vice dean of the faculty and from 2007 to 2009 he was the dean of the faculty of Electrical Engineering and Information Technology of RWTH Aachen University. His research interests are numerical field computation and optimization, the design and controls of electrical machines, in particular permanent magnet excited machines, induction machines and the design employing the methodology of virtual reality. Since several years Dr. Hameyer's work is concerned with the development of magnetic levitation for drive systems, magnetically excited audible noise in electrical machines and the characterization of ferromagnetic materials. Dr. Hameyer is author of more than 250 journal publications, more than 500 international conference publications and author of 4 books. Dr. Hameyer is a member of VDE, IEEE senior member, fellow of the IET.